Electronic Properties of Doped Molecular Thin Films Measured by Kelvin Probe Force Microscopy†

O. Tal and Y. Rosenwaks*

School of Electrical Engineering, Tel Aviv University, Tel Aviv 69978, Israel

Received: August 14, 2006; In Final Form: September 28, 2006

We report on high-resolution electronic measurements of doped organic thin-film transistors using Kelvin probe force microscopy. Measurements conducted on field effect transistors made of *N*,*N*′-diphenyl-*N*,*N*′-bis(1-naphthyl)-1,1′-biphenyl-4,4′-diamine p-doped with tetrafluoro-tetracyanoquinodimethane have allowed us to determine the rich structure of the doping-induced density of states. In addition, the doping process changes only slightly the Fermi energy position with respect to the highest occupied molecular orbital level center. The moderate change is explained by two counter-acting effects on the Fermi energy position: the doping-induced additional charge and the broadening of the density of states.

I. Introduction

The field of semiconducting organic molecular films is developing very fast, driven by the enormous potential demonstrated by these materials for applications in optoelectronics and inexpensive electronics such as light-emitting diodes, field effect transistors, and photovoltaic cells. As an example, organic thin-film transistors (OTFTs) present several possible advantages, such as low-cost processing, mechanical flexibility, and patterning for large-area applications. Improving the performance of OTFTs requires a deep understanding of charge carrier transport mechanisms through the organic layer. Although material technology advanced significantly over the last two decades, a fundamental understanding of the basic electronic and optical processes in these materials is still rather poor, and extensive research is necessary.

A good example of the above is the insertion of electronically active dopant molecules (i.e., electron donors or acceptors) into organic thin films, which has already been demonstrated by several groups. Dopants are introduced either intentionally to improve the film conductivity,[1] modify charge injection barriers,[2] add functionality (e.g., a pn junction[3]), and modify the film optical properties[4] or unintentionally as synthesis impurities[5], solution residuals,[6] and chemically induced doping,[7] which deteriorate the performance of the organic material. In any case, an accurate understanding of the density of states (DOS) energy distribution and how it is affected by molecular doping is one of the keys to advancing basic research on and technological applications of organic semiconductor films, since most electronic properties of organic semiconductors are closely related to the shape of the DOS[8,9]

In this work, we use high lateral resolution Kelvin probe force microscopy (KPFM) to measure several electronic properties of doped organic molecular thin films. KPFM has already been utilized for the study of charge mobility in OTFTs,[10] and the potential drops at the source and drain contacts of operating OTFTs.[11,12] Here, it is demonstrated that by using KPFM measurements across OTFT with a relatively thin organic film (10 nm) it is possible to measure quantitatively the energy distribution of the hole DOS and the Fermi level position.

II. Experimental Section

A typical OTFT structure used in all measurements is schematically shown in Figure 1. The OTFT substrates (fabricated by the Tessler group at the Technion−Israel Institute of Technology) consisted of a heavily doped p-type silicon gate electrode, a thermally grown 90 nm silicon oxide gate insulator, and 50-nm-thick gold strips evaporated on the oxide to form source and drain electrodes separated by 16 μm. A thin film (10 nm) of *N*,*N*′-diphenyl-*N*,*N*′-bis(1-naphthyl)-1,1′-biphenyl-4,4′-diamine (a-NPD) was deposited on the substrate by sublimation in an ultrahigh vacuum chamber. Doped a-NPD films were formed by coevaporation of tetrafluoro-tetracyanoquinodimethane (F_4TCNQ) with the host molecules (by the Kahn group at Princeton University). The OTFTs were transported under nitrogen atmosphere to a glovebox (<2 ppm H_2O) at Tel Aviv University in which the KPFM is located.

KPFM is used for high-resolution determination of the surface potential profile across the OTFT channel as shown schematically in Figure 1. The KPFM utilizes an atomic force microscope tip (Nanosensors, EFM; force constant: ∼2.8 N/m) as a probe electrode for measuring the contact potential difference (CPD) with a lateral resolution of tens of nanometers and an energy resolution of a few millielectronvolts. It is based on a commercial atomic force microscope (Autoprobe CP, Veeco, Inc.) operating in the noncontact mode (tip vibration amplitude: 20 nm; vibration resonance frequency: ∼75 kHz). An alternating voltage $V_{ac}\sin(\omega t)$ at a frequency of around 20 kHz was applied to the cantilever to induce an alternating electrostatic force between the tip and the sample. The CPD between the tip and the sample surface was measured by nullifying the output signal of a lock-in amplifier, which measures the electrostatic force at the frequency ω.[13−15] The transistors were scanned by KPFM while a semiconductor parameter analyzer (HP 4155C) was used to control the gate-source voltage (V_{GS}), with respect to the grounded source and drain electrodes, and monitor the drain, source, and gate electrode currents. The contact resistance,[16,17] leakage current through the gate insulator to the periphery of the active area, and shifts of the threshold voltage[16] due to

† Part of the special issue "Arthur J. Nozik Festschrift".

* Author to whom correspondence should be addressed. E-mail: yossir@eng.tau.ac.il.

10.1021/jp065246q CCC: $33.50
Published on Web 11/14/2006

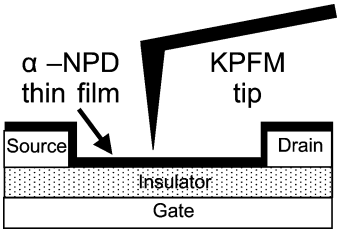

Figure 1. Schematic of the OTFT structure and KPFM tip above the channel.

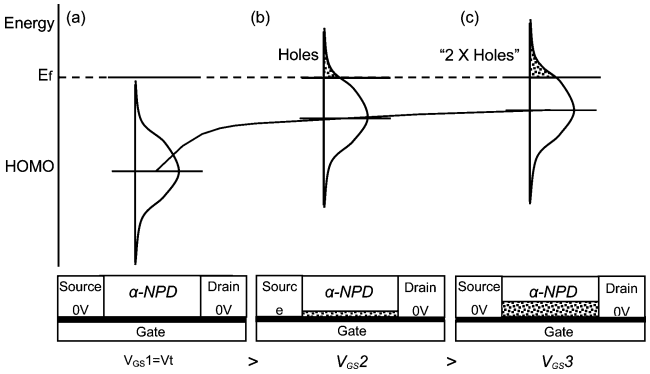

Figure 2. Top**:** Qualitative scheme of the hole occupation of a Gaussian DOS at different positions with respect to E_f. Bottom: OTFT cartoons in which the relevant charge concentration is represented by a dotted region. (a) $V_{GS}1 = V_t$, i.e., zero gate-induced hole concentration; (b) $V_{GS}2 < V_t$, thus holes accumulate to form a conducting channel; (c) $V_{GS}3 < V_{GS}2$ such that the hole concentration is twice that in part b.

continuous voltage application were found to be negligible in these transistor structures.

III. Results and Discussion

A. Density of States Measurements. We use the transistor structure to control the hole concentration by applying different V_{GS} values while measuring the level shift with KPFM, as shown schematically in Figure 2. Assuming a Gaussian distribution of the DOS related to the highest occupied molecular orbital (HOMO), when $V_{GS} = V_t$ (V_t is the threshold voltage defined as the V_{GS} at the onset of the conduction channel) there is no induced charge in the organic film, and the DOS is located below the Fermi energy level. However, when $V_{GS} < V_t$, holes are injected into the organic film from the grounded source and drain electrodes to screen the gate negative charge. The holes populate the tail states of the HOMO DOS, and the molecular energy levels shift toward the Fermi energy as shown (solely for the HOMO) in Figure 2b. During the measurement, the Fermi energy is kept constant by the grounded source and drain contacts, and the molecular energy levels are shifted with respect to the Fermi energy by the gate-induced voltage. When $|V_{GS}|$ is further increased (Figure 2c) such that twice as many holes are injected into the film than in the former case, the HOMO energy levels are shifted less than before because there are more states available as the DOS is larger near the Fermi Level. The above description illustrates the relation between the charge concentration and the HOMO shift to the specific shape of the DOS: A low state density results in a larger HOMO shift for a certain increase of hole concentration, while at a higher state density the HOMO shift is smaller for the same increase in hole concentration.

Assuming negligible level bending the shift of the energy levels ($-qV_L$, where q is the elementary charge) for different V_{GS} values with respect to the level position at $V_{GS} = V_t$ can be measured directly by KPFM

$$V_L(x) \equiv \mathrm{CPD}(x) - \mathrm{CPD}_t(x) \tag{1}$$

where CPD(x) is the contact potential difference measured between the KPFM tip and the sample at a given location x across the transistor (Figure 3) and $\mathrm{CPD}_t(x)$ is measured at $V_{GS} = V_t$. Figure 3 shows a qualitative energy level scheme across a KPFM-measured OTFT far from the source and drain contacts for (a) negligible and (b) nonnegligible level bending. In part a when the applied gate-source voltage $V_{GS} = V_t$ and the drain-source voltage $V_{DS} = 0$ V (solid curves), there is no charge injection into the channel and no level shift in the organic film, i.e, $V_L(x) = \mathrm{CPD}(x) - \mathrm{CPD}_t(x) = 0$. When $V_{GS} < V_t$ and $V_{DS} = 0$ V (dashed curves), holes are injected into the channel, and $V_L(x) = \mathrm{CPD}(x) - \mathrm{CPD}_t(x) > 0$. In the case of nonnegligible level bending (Figure 3b), the measured $V_L(x)$ is smaller because part of the applied gate voltage induces band bending in the organic layer.

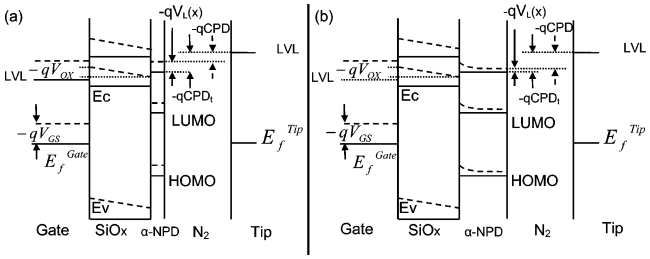

Figure 3. Qualitative energy level scheme across a OTFT measured by KPFM far from the source and drain contacts for $V_{GS} = V_t$ and $V_{DS} = 0$ V (solid curves) and $V_{GS} < V_t$ and $V_{DS} = 0$ V (dashed curves) in the case of (a) negligible and (b) nonnegligible level bending. In the second case (b), the measured $V_L(x)$ is smaller because part of the applied gate voltage induces band bending in the organic layer.

Our method for DOS measurement is feasible when the energy level bending perpendicular to the gate can be neglected. According to our numerical calculations[18] conducted for a 10-nm-thick organic layer in an OFET structure and different Gaussian DOS distributions, the induced charge is homogeneously distributed across the organic film width, and the energy level bending from the film surface to the film/gate insulator interface is negligible up to a certain V_{GS} value. Above this given V_{GS} value,[19] the conducting channel is squeezed toward the gate insulator, and the level bending is not negligible; this behavior has already been reported elsewhere.[20,21] Under negligible level bending conditions, the shift of the energy levels (V_L) for different V_{GS} values with respect to the level position at $V_{GS} = V_t$ can be measured directly by KPFM based on eq 1.

The hole concentration at any lateral location x in the channel is given by

$$p(x) = -\frac{C_{OX}}{qd_{org}}(V_{GS} - V_t - V_L(x)) \tag{2}$$

where C_{OX} is the silicon oxide (insulating layer) capacitance per unit area and d_{org} is the organic film thickness. Equation 2 is only valid when the charge concentration is homogeneously distributed across the organic film depth. However, the hole concentration in the channel is given by

$$p = \int_{-\infty}^{\infty} g(E)(1 - f_{FD}(E))\,\mathrm{d}E \tag{3}$$

where $g(E)$ is the DOS relevant for holes and $f_{FD}(E)$ is the Fermi−Dirac distribution. With the hole concentration and the energy level shift, the hole DOS is calculated as described in

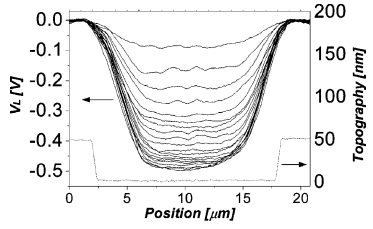

Figure 4. Topography curve (bottom) and V_L curves (top) measured by KPFM across the transistor top surface for $V_{DS} = 0$ V and -16.5 V $\leq V_{GS} \leq 0$ V.

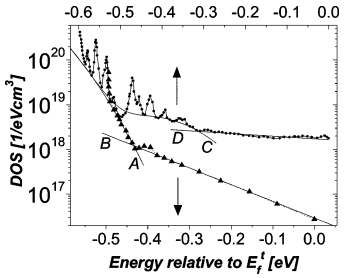

Figure 5. DOS vs energy relative to E_f^t (E_f at $V_{GS} = V_t$) for undoped (solid triangles) and doped (solid circles) samples. The solid curves are fittings of a Gaussian function (eq 2, curve A) and an exponential function (eq 4, curve B) to given ranges in the undoped sample DOS curve and a fitting of eq 3 (curve C) to the doped sample DOS curve.

Appendix A to give

$$g(qV_L(x)) = \frac{C_{OX}}{d_{org}q^2}\left(\frac{dV_{GS}}{dV_L(x)} - 1\right) \quad (4)$$

This analytic expresion, which has no fitting parameters, is used to obtain the DOS from the measured V_L.

Figure 4 shows V_L (solid curves) and topography (dashed curve) profiles measured simultaneously across an undoped transistor. The protruding regions on the left and right sides of the bottom topography profile correspond to the source and drain contacts, while the conduction channel is located between them (see Figure 1 for comparison). The potential of the grounded source and drain appears as the flat portion at each end of the V_L curves, and the potential distribution across the organic channel is seen between them. The V_L curves were measured for V_{GS} values ranging from 0 to -16.5 V across relatively smooth regions of the organic layer (roughness, <1 nm).

The DOS calculated using eq 4 is plotted versus qV_L in Figure 5 for undoped (triangles) and doped (circles) samples (doping concentration, $N_a = 1.4 \times 10^{18}$ cm^{-3} [22]). Each DOS curve is based on an average of 50 sets of V_L curves similar to the one in Figure 4. The sets were measured at different locations on the transistors to reduce the experimental uncertainty. The energy scale in Figure 5 represents the energy relative to E_f^t, defined as the E_f position at $V_{GS} = V_t$, and the negative sign denotes values below E_f^t. The sharp increase in DOS near the high-energy end of the curves (left side of Figure 5) reflects the termination of the level shift, possibly due to the failure of the negligible level bending assumption at the corresponding V_{GS} value or due to the Fermi level pinning phenomenon. The rich DOS structure has been discussed in detail by us recently;[22] in short, the sharp peaks observed in the doped sample may imply the presence of several doping-induced energy levels, and the differences in the general curve shapes were ascribed to a broadening of the DOS due to the presence of dopants.

B. Fermi Level Position. The Fermi energy position is subjected to two counteracting effects due to the introduction of dopants into the molecular film. According to Bassler et al.,[23] holes can be transferred from the dopant's lowest unoccupied molecular orbital (LUMO) to the host HOMO even if the dopant LUMO is ~0.8 eV below the HOMO level of the host material. This is due to stabilization by Coulomb interactions between ionized dopants and released holes localized in nearby hopping sites. In our case $HOMO_{host} - LUMO_{dopant} \cong 0.28$ eV;[24] thus all of the dopants are most likely ionized under equilibrium conditions. As illustrated schematically by Figures 6a and 6b, respectively, the dopant-induced increase in the hole concentration shifts E_f^t from its original position ($E_{f_a}^t$) in the undoped sample toward the HOMO center (position $E_{f_b}^t$). This shift (-0.535 eV) was calculated by finding the lower limit $E_{f_b}^t$ of an integral on the measured DOS in the undoped sample that equals the dopant-induced hole concentration (p_{doping})

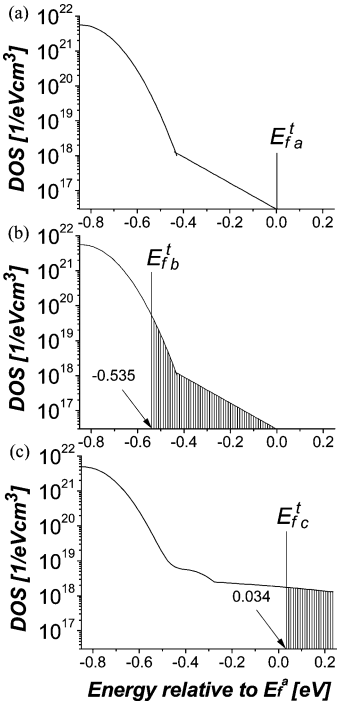

Figure 6. Schematic representation of the chemical potential and the position of the DOS edge for three cases: (a) undoped sample, where "0 eV" denotes the E_f^t position at the beginning of the DOS measurement (i.e., at $V_{GS} = V_t$); (b) hypothetical case of the undoped DOS populated by the dopant-induced holes (states occupied by holes appear as the shaded region); (c) doped sample. The DOS shape is represented by function fits to the measured DOS (Figure 5, curves A and B for the undoped case and curves C and D for the doped case, respectively).

$$p_{doping} = N_a = 1.4 \times 10^{18}\ \text{cm}^{-3} = \int_{E_{f_b}}^{0} g(E)_{undoped}(1 - f_{FD}(E))\, dE \quad (5)$$

However, as measured and shown in the previous section, dopants induce a DOS broadening or conversion of shallow states into deep states in the HOMO−LUMO gap as schematically shown in Figure 6c. This effect should shift E_f^t away from the HOMO center; on the basis of the fitting of Gaussian functions to the measured DOS,[22] the HOMO DOS centers of the doped and the undoped samples are located at $E_c = -0.88 \pm 0.04$ eV, and the E_f^t shift from the undoped sample to the doped sample is only 34 meV from the HOMO center ($E_{f_c}^t$ position). Thus, in this case, the broadening of the HOMO level is compensating for the Fermi level shift induced by the dopants, as shown in

Figure 6c. This phenomenon is unique in comparison with crystalline inorganic semiconductors, where the DOS does not change upon doping and the introduction of p-type dopants causes E_f^t to shift toward E_c, the valance band edge.

From a technological point of view, any addition of doping or presence of impurities that act as dopants have a substantial effect on the DOS and consequently on the position of the Fermi level energy. This has important consequences on the physics and operation of all organic-based devices.

IV. Conclusions

The KPFM-based method described here allowed the direct determination of the DOS distribution in a molecular film and the effect of doping on this distribution. The dopant molecules broaden the DOS and induce several discrete peaks on the main distribution. In addition, the doping process changes only slightly the Fermi energy position with respect to the HOMO center due to two counteracting effects on the Fermi energy position: the doping-induced additional charge and the broadening of the DOS. Future DOS measurements of specific organic layers with several different doping concentrations are expected to provide additional information on doping-induced effects such as internal electrostatic screening.

Acknowledgment. This research was generously supported by the U. S.−Israel Binational Science Foundation (Grant No. 2000-092). The authors thank N. Tessler (Technion, Israel) and A. Kahn (Princeton University, Princeton, NJ) for supplying the samples for this research and for very fruitful discussions.

Appendix: Extraction of Density of States

If we define E_f^t as the Fermi energy level position for $V_{GS} = V_t$ and $V_{DS} = 0$ V, then qV_L is the shift of the quasi-Fermi level E_f^q with respect to E_f^t. (Recall that qV_L also equals the electronic level shift with respect to their position at $V_{GS} = V_t$ and $V_{DS} = 0$ V.) Taking the derivative of the hole concentration (eq 3) with respect to V_L we obtain

$$\frac{dp}{dV_L} = \int_{-\infty}^{\infty} g(E) \frac{df_{FD}(E)}{dV_L} dE \tag{A.1}$$

where the Fermi−Dirac distribution is given by

$$f_{FD}(E,V_L) = \frac{1}{1 + \exp\left(\frac{E - E_f^t - qV_L}{kT}\right)} \tag{A.2}$$

So the derivative in eq A.1 becomes

$$\frac{df_{FD}(E,V_L)}{dV_L} = \frac{q}{kT} \frac{\exp\left(\frac{E - E_f^t - qV_L}{kT}\right)}{\left[1 + \exp\left(\frac{E - E_f^t - qV_L}{kT}\right)\right]^2} \tag{A.3}$$

When the width of df_{FD}/dV_L is much narrower relative to that of $g(E)$ it can be approximated by a δ function

$$\frac{\exp\left(\frac{E - E_f^t - qV_L}{kT}\right)}{\left[1 + \exp\left(\frac{E - E_f^t - qV_L}{kT}\right)\right]^2} = \delta\left(\frac{E - E_f^t - qV_L}{kT}\right) \tag{A.4}$$

Inserting eqs A.3 and A.4 into eq A.1 we obtain

$$\frac{dp}{dV_L} = \frac{q}{kT} \int_{-\infty}^{\infty} g(E)\delta\left(\frac{E - E_f^t - qV_L}{kT}\right) dE \tag{A.5}$$

Using

$$\delta\left(\frac{x}{a}\right) = a\delta(x) \tag{A.6}$$

we obtain

$$\frac{dp}{dV_L} = q \int_{-\infty}^{\infty} g(E)\delta(E - E_f^t - qV_L)\, dE \tag{A.7}$$

and using

$$\int f(x)\delta(x - a)\, dx = f(a) \tag{A.8}$$

we obtain

$$\frac{dp}{dV_L} = qg(E_f^t + qV_L) \tag{A.9}$$

Thus the DOS can be expressed as a function of qV_L as

$$g(E_f^t + qV_L) = \frac{1}{q} \frac{dp}{dV_L} \tag{A.10}$$

By applying eq A.10 to eq 2 we obtain eq 4, which is used to obtain the DOS from the measured V_L.

References and Notes

(1) Shen, Y.; Diest, K.; Man, H. W.; Hsieh, B. R.; Dunlap, D. H.; Malliaras, G. G. *Phys. Rev. B* **2003**, *68*, 081204.
(2) Gross, M.; Muller, D. C.; Nothofer, H. G.; Scherf, U.; Neher, D.; Brauchle, C.; Meerholz, K. *Nature* **2000**, *405*, 661.
(3) Qibing, P.; Gang, Y.; Chi, Z.; Yang, Y.; Heeger, A. J. *Science* **1995**, *269*, 1086.
(4) Welter, S.; Brunner, L.; Hofstraat, J. W.; De Cola, L. *Nature* **2003**, *421*, 54.
(5) Naka, S.; Okada, H.; Onnagawa, H.; Yamaguchi, Y.; Tsutsui, T. *Synth. Met.* **2000**, *111*, 331.
(6) Sakai, K.; Ikezaki, K. In *Proceedings of the 11th International Symposium on Electrets: ISE11*; 2002; 151.
(7) Honhang, F.; Kachu, L; Shukong, S. *Jpn. J. Appl. Phys., Part 2* **2002**, *41*, L1122.
(8) Arkhipov, V. I.; Heremans, P.; Emelianova, E. V.; Adriaenssens, G. J.; Bassler, H. *J. Phys.: Condens. Matter* **2002**, *14*, 9899.
(9) Koehler, M.; Biaggio, I. *Phys. Rev. B* **2003**, *68*, 752051.
(10) Burgi, L.; Sirringhaus, H.; Friend, R. H. *Appl. Phys. Lett.* **2002**, *80*, 2913.
(11) Burgi, L.; Richards, T. J.; Friend, R. H.; Sirringhaus, H. *J. Appl. Phys.* **2003**, *94*, 6129.
(12) Puntambekar, K. P.; Pesavento, P. V.; Frisbie, C. D. *Appl. Phys. Lett.* **2003**, *83*, 5539.
(13) Leng, Y.; Williams, C. C.; Su, L. C.; Stringfellow, G. B. *Appl. Phys. Lett.* **1995**, *66*, 1264.
(14) Kikukawa, A.; Hosaka, S.; Imura, R. *Appl. Phys. Lett.* **1995**, *66*, 3510.
(15) Shikler, R.; Meoded, T.; Fried, N.; Rosenwaks, Y. *Appl. Phys. Lett.* **1999**, *74*, 2972.
(16) Horowitz, G.; Lang, P.; Mottaghi, M.; Aubin, H. *Adv. Funct. Mater.* **2004**, *14*, 1069.
(17) Burgi, L.; Sirringhaus, H.; R. H. Friend. *Appl. Phys. Lett.* **2002**, *80*, 2913.
(18) Tal, O.; Tessler, N. Unpublished work.
(19) Approximately $V_{GS} \leq -3.5$ V and $V_{GS} \leq -15.6$ V for undoped and doped samples, respectively.
(20) Horowitz, G.; Hajlaoui, R.; Delannoy, P. *J. Phys. III* **1995**, *5*, 355.
(21) Horowitz, G.; Hajlaoui, R.; Bouchriha, H.; Bourguiga, R.; Hajlaoui, M. *Adv. Mater.* **1998**, *10*, 923.
(22) Tal, O.; Preezant, Y.; Tessler, N.; Chan, C. K.; Kahn, A.; Rosenwaks, Y. *Phys. Rev. Lett.* **2005**, *95*, 256405.
(23) Bassler, H. *Phys. Status Solidi B* **1993**, *175*, 15.
(24) Gao, W.; Kahn, A. *J. Appl. Phys.* **2003**, *94*, 359.